



Deposited via The University of Sheffield.

White Rose Research Online URL for this paper:

<https://eprints.whiterose.ac.uk/id/eprint/752/>

Conference or Workshop Item:

Lewis, R., Dwyer-Joyce, R.S., Olofsson, U. et al. (2004) Wheel material wear mechanisms and transitions. In: 14th International Wheelset Congress, 17-21 October, Orlando, USA. (Unpublished)

Reuse

Items deposited in White Rose Research Online are protected by copyright, with all rights reserved unless indicated otherwise. They may be downloaded and/or printed for private study, or other acts as permitted by national copyright laws. The publisher or other rights holders may allow further reproduction and re-use of the full text version. This is indicated by the licence information on the White Rose Research Online record for the item.

Takedown

If you consider content in White Rose Research Online to be in breach of UK law, please notify us by emailing eprints@whiterose.ac.uk including the URL of the record and the reason for the withdrawal request.



Wheel Material Wear Mechanisms and Transitions

R. Lewis^{1*}, R.S. Dwyer-Joyce¹, U. Olofsson², R.I. Hallam¹

¹Department of Mechanical Engineering, The University of Sheffield, Mappin Street, Sheffield, S1 3JD, UK, roger.lewis@sheffield.ac.uk, tel. +44 114 2227838, fax. +44 114 2227890.

²Department of Machine Design, KTH, SE 100 44 Stockholm, Sweden.

*Corresponding author

Summary: In order to develop more durable wheel materials to cope with the new specifications being imposed on wheel wear, a greater understanding is needed of the wear mechanisms and transitions occurring in wheel steels, particularly at higher load and slip conditions.

In this work wear assessment of wheel materials is discussed as well as wear rates, regimes and transitions. Twin disc wear testing, used extensively for studying wear of wheel and rail materials, has indicated that three wear regimes exist for wheel materials; *mild*, *severe* and *catastrophic*. These have been classified in terms of wear rate and features. Wear rates are seen to increase steadily initially, then level off, before increasingly rapidly as the severity of the contact conditions is increased. Analysis of the contact conditions in terms of friction and slip has indicated that the levelling off of the wear rate observed at the first wear transition is caused by the change from partial slip to full slip conditions at the disc interface. Temperature calculations for the contact showed that the large increase in wear rates seen at the second wear transition may result from a thermally induced reduction in yield strength and other material properties.

Wear maps have been produced using the test results to study how individual contact parameters such as load and sliding speed influence wear rates and transitions. The maps are also correlated to expected wheel/rail contact conditions.

This improved understanding of wheel wear mechanisms and transitions and will help in the aim of eventually attaining a wear modelling methodology reliant on material properties rather than wear constants derived from testing.

Index Terms: wheel steel, wear mechanisms

1. INTRODUCTION

New specifications are being imposed on railway wheels that are leading to an increase in the severity of the wheel/rail contact conditions [1]. This will increase the likelihood of wear occurring. Excessive wear can affect the dynamic behaviour of the railway vehicle and reduce ride comfort; impact upon the potential for derailment and reduce the integrity of the wheel material [2].

In order to deal with these demands new wheel materials are being developed to give greater durability. To aid such development an improved understanding is required of the wear mechanisms and regimes apparent in wheel steels.

As well as materials, new design tools are also being developed that incorporate vehicle dynamics and wear modelling for predicting the evolution of wheel profiles [2, 3, 4, 5, 6]. The two main drawbacks in some of these analysis tools are in the contact mechanics method used and the approach to wear modelling. Telliskivi and Olofsson [7, 8] studied different contact mechanics methods used in wear simulations and concluded that they significantly affected the accuracy. They also developed a new method with increased accuracy and no loss of calculation speed. Previously developed wear models are taken in most cases, based on the Archard sliding wear model or a frictional work model, and used with wear coefficients taken from the literature. It is apparent in each case that the detail and accuracy of the dynamic modelling far exceeds that of the wear modelling. The approach used by Lewis et al. [6] has led to an improved model, but it is still reliant on wear coefficients derived from twin disc testing. Ideally a model based on material properties is required. In order to achieve this and improved the design tools, a clearer understanding of the wheel steel wear mechanisms is needed.

The aim of this paper is to draw together current understanding of the wear mechanisms, regimes and transitions and identify gaps in the knowledge and to develop new tools for assessing wear of wheel materials, such as wear maps, that can be used to improve wear prediction.

2. WEAR MECHANISMS IN WHEEL MATERIALS

A number of different techniques have been used for studying wear of railway wheel steels. Field measurements have been used in the past to study the causes of wheel and rail wear [9]. A large amount of data has also been gathered from simulated field experiments carried out on specially built test tracks [10]. Laboratory methods used range from full-scale laboratory experiments [11] and scaled-down tests [12] to bench tests using a twin disc set-up [13, 14, 15, 16, 17]. The twin disc approach has been used more than most because it offers greater control over experimental variables as well as the ability to test a wide range of materials at lower cost. All the data presented in this paper was generated using such tests.

Early twin disc test work carried out to study the wear behaviour of railway wheel steels led to the identification of two wear regimes [13, 14]. These were designated *mild* and *severe*. Later work led to the identification of a third regime, beyond the originally identified severe regime, designated *catastrophic* wear [15]. It was thought likely that wheel tread wear would fall within the mild regime while flange wear would be in the severe or catastrophic regime.

The regimes were characterised in terms of wear rate and wear debris. There was, however, no detailed analysis of the wear mechanisms occurring within the regimes and no understanding has been gained as to why the regimes exist.

More recent work has led to a greater understanding of the wear mechanisms and transitions [18]. These studies were carried out using a twin disc approach and a relatively new wheel material, R8T. Wear rates were plotted in a similar manner to previous work [13, 14, 15]. An energy approach was adopted in the analysis of the relationship between wear rate and contact conditions by relating wear rate (mg/m rolled) to $T\gamma$, where T is the tractive force, γ is the slip. For mild contact conditions it was shown that wear rate is proportional to $T\gamma$, in agreement with previous studies [15] (see Figure 1). Results from the full range of contact conditions tested, however,

show that as contact severity increases and wear transitions occur this relationship breaks down (see Figure 2).

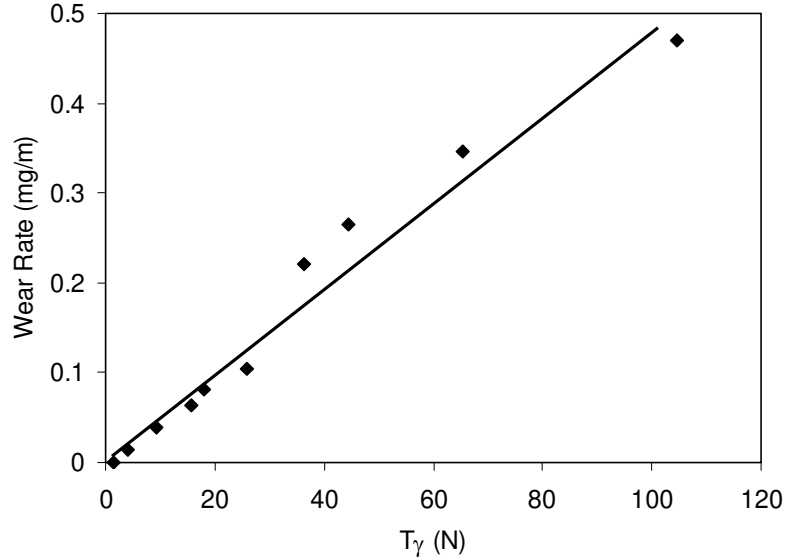


Figure 1. R8T Wear Rates for Mild Contact Conditions (data from [18])

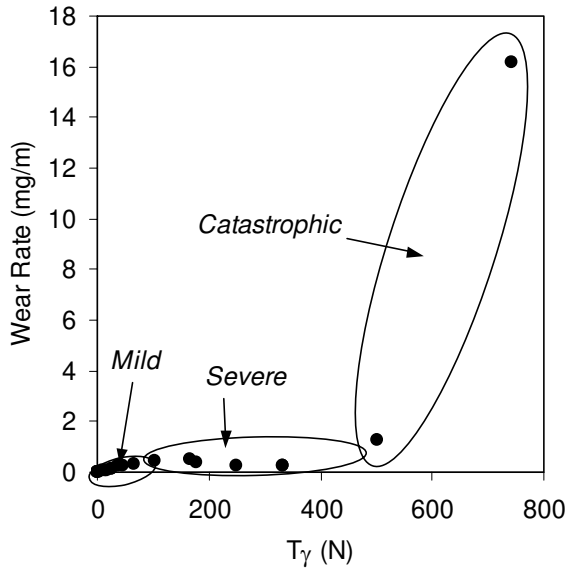


Figure 2. R8T Wheel Steel Wear Rates and Regimes (from [18])

At low T_γ , in the mild wear regime, oxidative wear was seen to occur on both wheel and rail discs. The disc surfaces turned a rusty brown colour. Closer examination of the wear surface of the wheel disc revealed abrasive score marks and evidence of the oxide layer breaking away from the surface (see Figure 3a). This ties in with observations made in the field that on straight track where low slip occurs on the high rail, oxidative wear is prevalent generating magnetite (Fe_3O_4) [19] and in full-scale test-rig results, where reddish oxide film appeared for low slip conditions [11]. As T_γ was increased, the wear mechanism of the wheel discs altered. The wheel disc appeared to be wearing by a ratchetting process (deformation followed by crack growth and subsequent material removal). Closer examination of the wheel disc surfaces revealed that this was the case (see Figure 3b).

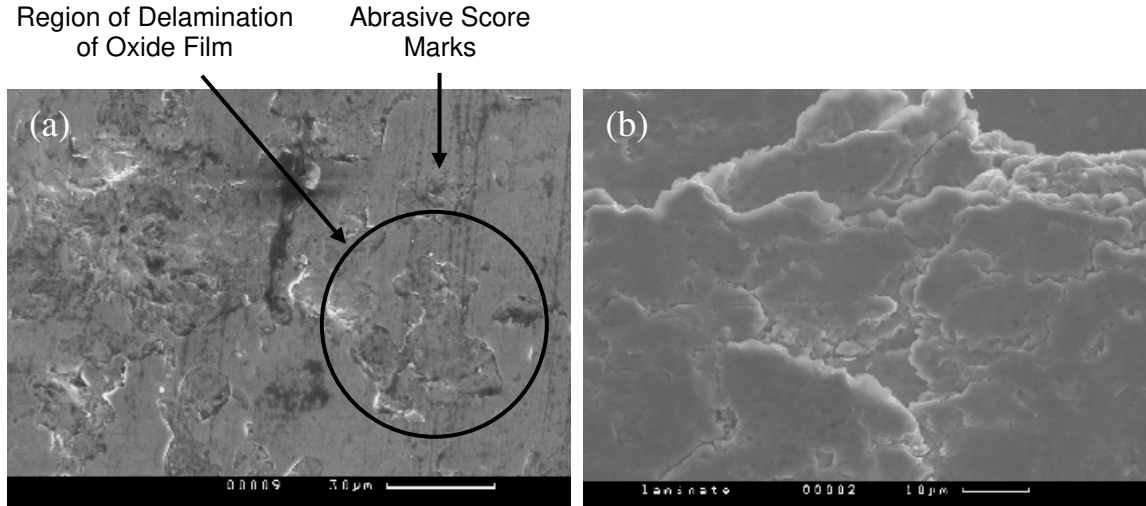


Figure 3. Wheel Disc Surface Run at (a) $T\gamma = 1.3$ and (b) $T\gamma = 26.0$.

Figure 4a shows a section through a wheel disc, run at low $T\gamma$, parallel to the rolling direction. At the surface the oxide layer is just visible. There is a very small amount of deformation just below the wear surface of the disc.

At higher levels of $T\gamma$, observation of the subsurface morphologies revealed that a larger amount of plastic deformation was occurring below the wheel disc wear surface (see Figure 4b) and crack formation just below the surface was visible which was leading to thin slivers of material breaking away from the surface. The slivers have a similar thickness to the oxide layer and could indicate a severe oxidative wear mechanism is occurring, where fracture occurs between the oxide layer and the metal.

As $T\gamma$ was increased further far greater cracking was visible at the wear surface and some of these cracks were seen to alter direction from running parallel to the wear surface and turning up to turning down into the material causing larger chunks of material to break away (see Figure 4c).

3. WEAR TRANSITIONS

3.1 Limiting Traction

Figure 5 shows how the different wear features observed relate to the wear rates and regimes observed in the results of the twin disc testing with R8T wheel material and UIC60 900A rail steel. At low $T\gamma$ wear appears to be dominated by surface oxidation and at high $T\gamma$ the wear is dominated by surface cracking and mass loss by spalling. In order to further understand the wear mechanisms, the transitions between these regimes were studied in more detail. It was proposed that the first transition is associated with the onset of fully sliding contact conditions and the second is a result of surface temperature effects.

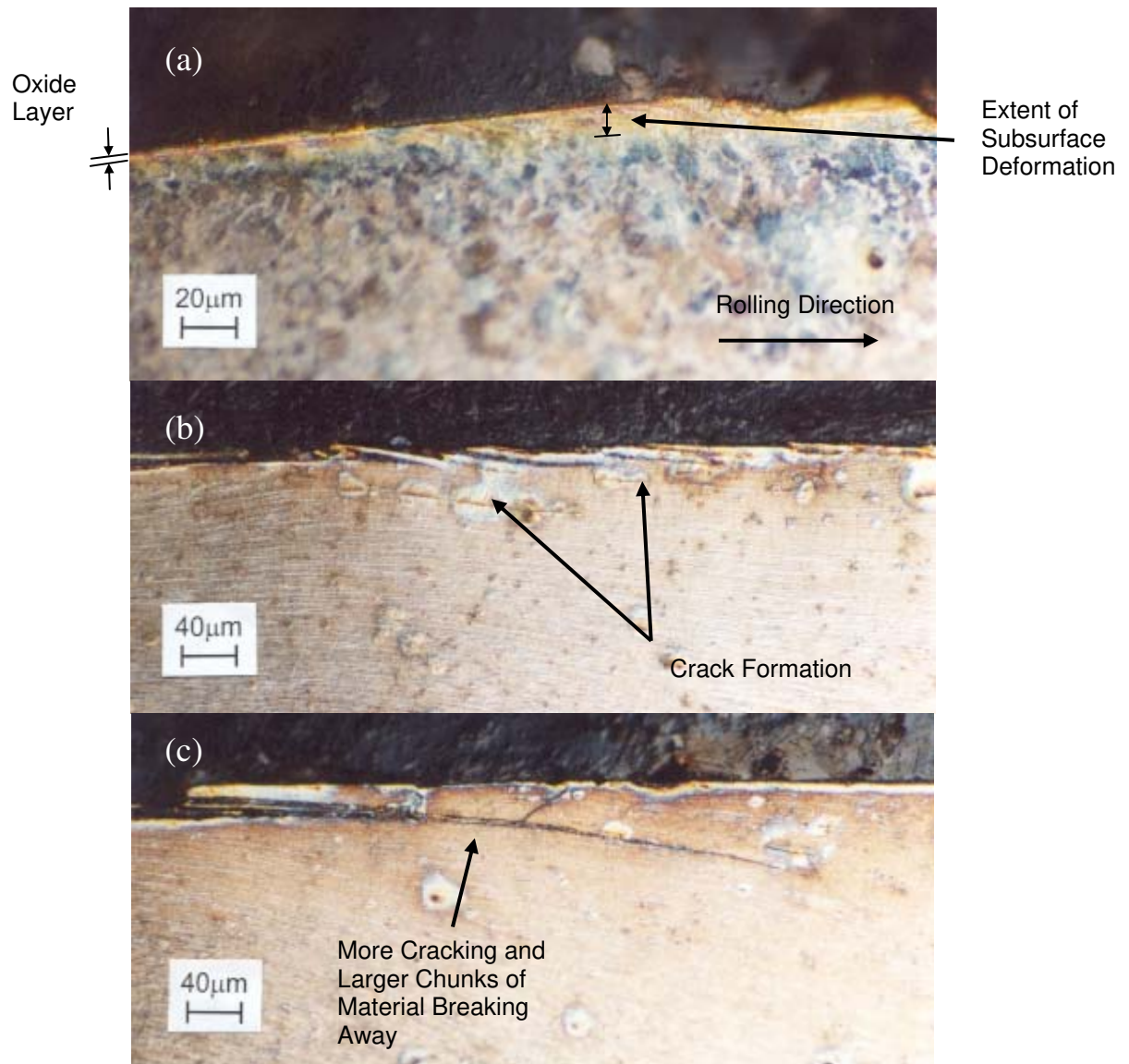


Figure 4. Sections Parallel to Rolling Direction through Wheel Disc Run at: (a) $T\gamma = 1.3$; (b) $T\gamma = 104.5$ and (c) $T\gamma = 166.8$

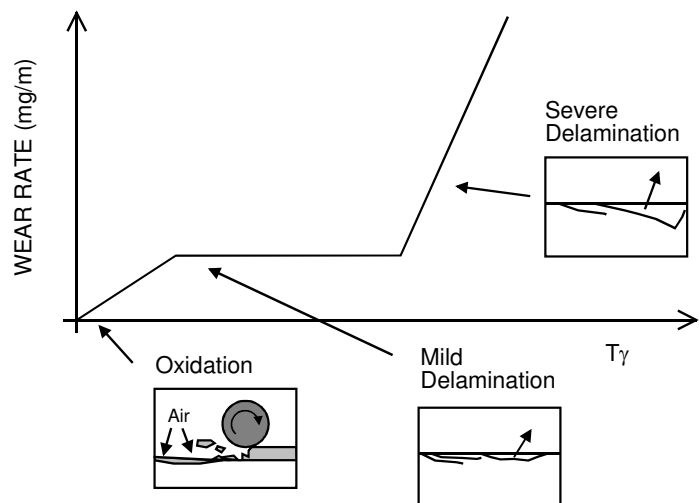


Figure 5. Schematic Diagram of Wear Features and Regimes

Figure 6 shows friction measurements taken during R8T wear tests carried out at 1500MPa plotted against slip, i.e. a creep curve. As would be expected the friction reaches a threshold. This transition represents the change from partial slip in the disc interface to full slip conditions. Also shown is the Carter creep curve for an assumed limiting friction of 0.5. This model creep curve is based on smooth elastic cylinders in contact [20].

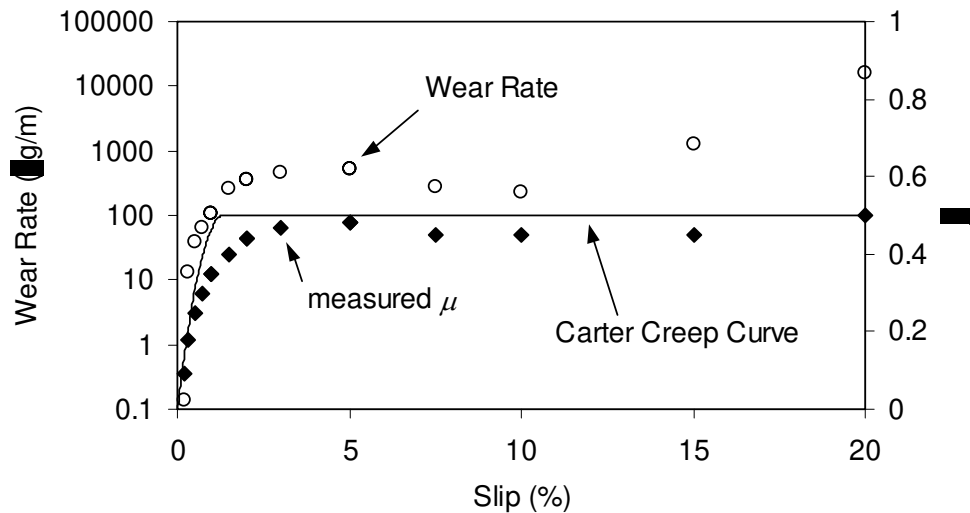


Figure 6. Friction versus Slip in the Twin Disc Contact (for tests carried out at 1500MPa)

The wear data (also shown in Figure 6) follows a similar pattern indicating that at the point of transition from partial slip to full slip a wear transition also occurs. After the full slip condition has been reached, increasing the magnitude of slip has no effect. As shown in Figure 7, depth of plastic deformation (from sections of test discs) follows a similar pattern with respect to slip.

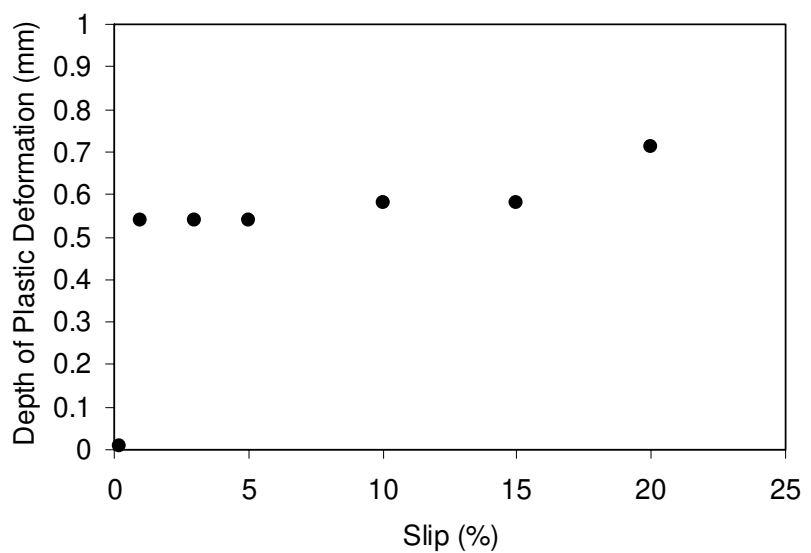


Figure 7. Depth of Sub-Surface Plastic Deformation against Slip for R8T Wheel Material (for twin disc tests carried out at 1500MPa)

As slip is increased the traction distribution in the contact, q , increases (whilst $q < \mu p$). The shear stress at the surface thus increases, which results in increasing wear with slip. Once limiting friction has been reached ($q = \mu p$ everywhere in the contact region) then the surface shear stress remains constant with increasing slip. This explains the plateau shown in Figure 6. The wear is largely independent of sliding velocity. This is an interesting observation because it suggests that, in this regime, the wear is controlled by contact stress and limiting traction alone. If the wear mechanism had been by abrasion (for example caused by asperities or hard particles abrading the surface) then increasing the sliding velocity would result in proportionally more abrasive ploughing and wear. In this regime it is therefore reasonable to model the material removal process using a contact mechanics model such as those proposed previously [21]. The contact stress causes an increment of shear strain, which accumulates (ratchets) until the material ruptures [22].

3.2 Thermal Softening

At the second wear transition (where the wear data breaks from the pattern of the friction measurements) another mechanism must be initiated, leading to the much higher wear rates observed. Once the slip has reached about 15% the wear rate increases rapidly. The theoretical smooth surface stress state, however, remains unaltered since the normal load and traction coefficient are unchanged. Clearly the increase in sliding speed has resulted in some mechanism changes. In this section the associated surface temperature rise is considered.

An approach for determining the temperature in a twin disc experimental contact has been outlined previously [18]. The disc surface temperature is considered to be made up of three components:

1. The body temperature, T_b , of the material under the contacting surfaces of the discs, which is the average temperature of the outer surface of the discs.
2. The instantaneous temperature rise above the bulk temperature at the point of contact, called the flash temperature, T_f [23].
3. The ambient temperature of the air surrounding the discs, T_a .

In order to calculate the body (or average surface temperature) of the two discs in contact, T_b , heat generated due to sliding friction in the contact is equated to heat loss due to convection, conduction and radiation giving:

$$\mu F_n u_s = 2(\mathcal{Q}_1 + \mathcal{Q}_2 + \mathcal{Q}_3) \quad (1)$$

where μ is the coefficient of friction, F_n is the normal load applied to the discs, u_s is the sliding speed and \mathcal{Q}_1 , \mathcal{Q}_2 and \mathcal{Q}_3 are heat loss due to convection, conduction and radiation respectively. The dissipated heat is multiplied by two as there are two discs.

Calculations were carried out to determine temperatures in the twin disc contact for R8T versus UIC60 900A rail steel. The results, shown in Figure 8, indicate that the transition from severe to catastrophic wear occurs between 200°C and 300°C. These temperatures correspond with those causing a drop in the yield strength of carbon manganese steels similar to wheel and rail steels [24].

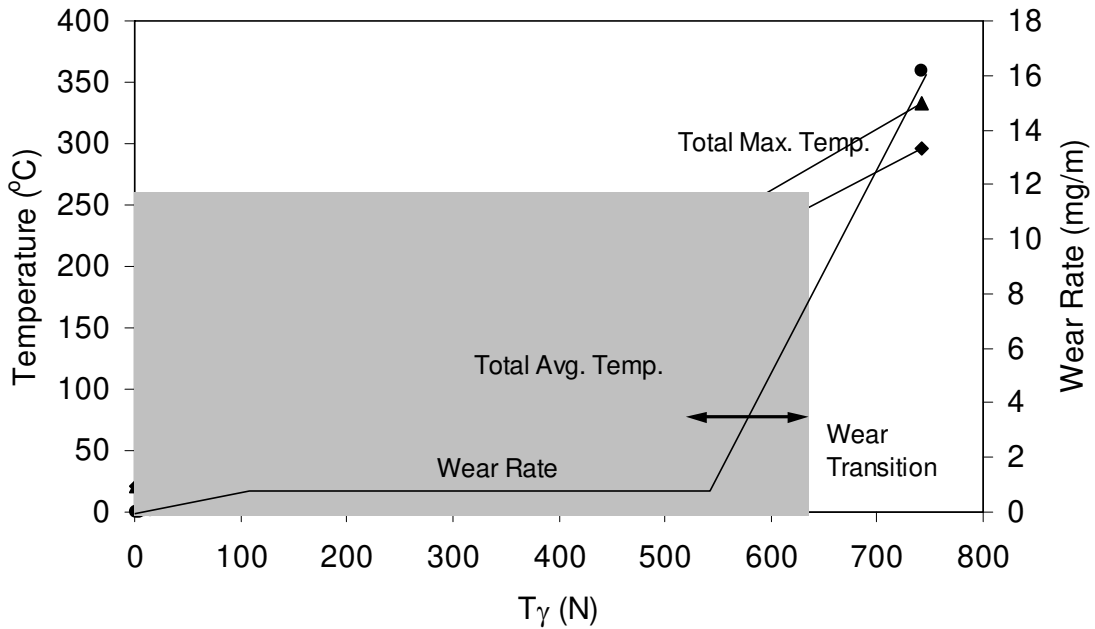


Figure 8. Disc Contact Temperatures varying with Slip and Compared with Wear Rates

4. WEAR MAPPING

While using the T_γ method for plotting wear rate data enables wear transitions to be identified easily and comparisons of different material combinations to be made it does not help in fully understanding how the individual contributions of different parameters such as contact pressure and slip affect wear rate.

In order to allow a more complete analysis of the effect of individual parameters a mapping method was used for plotting wear data. The approach used was similar to that developed by Lim and Ashby [25] for mapping sliding wear mechanisms and previously used for studying rail steel wear transitions by Lewis & Olofsson [26]. Wear coefficients were calculated from the wheel steel wear data using Archard's equation [27]:

$$K = \frac{Vh}{Pd} \quad (2)$$

where K is the wear coefficient, V is the wear volume, P is the normal load, d is the sliding distance and h is the material hardness.

Wear coefficients were then plotted against contact pressure and sliding speed in the contact. Two types of plots were constructed; contour maps and 3D point graphs. Obviously the accuracy of the contour map is limited by the amount of data available. The accompanying 3D graphs give an indication of where data is lacking on a particular map. Transitions based on those outlined above were marked on the contour plots.

Figure 9 illustrates data from twin disc testing using Class D Tyre versus BS11 rail material (details in [15]). Data was available at high sliding velocities giving a good picture of wear likely under severe wheel/rail contact conditions. Figure 10 shows data from twin disc testing for R8T wheel material versus UIC60 900A rail (for details see [18]).

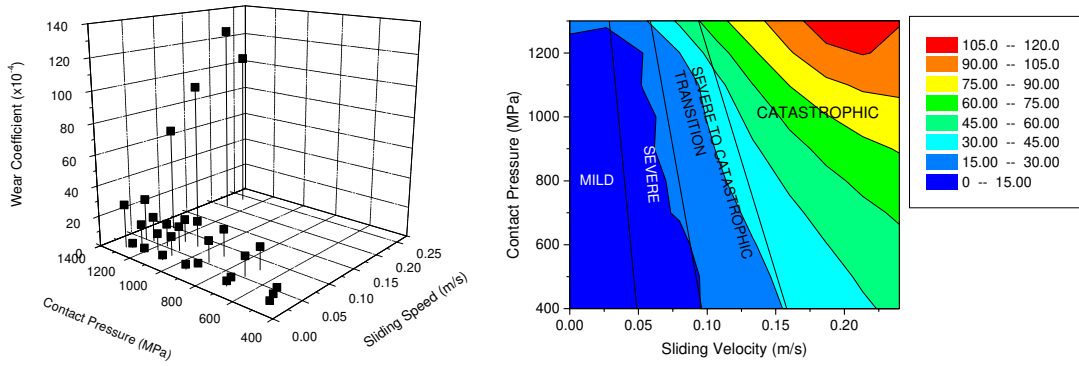


Figure 9. Wear Coefficient Maps for Class D Tyre Material versus BS11 Rail Material (data from Bolton & Clayton, (1984))

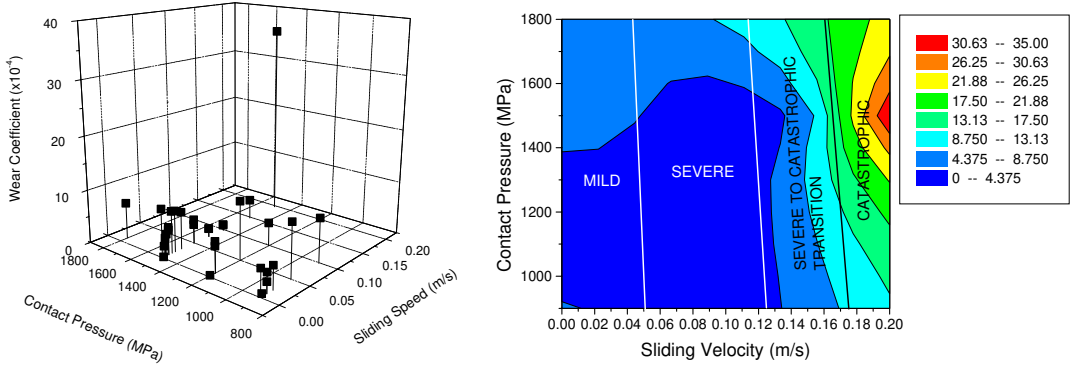


Figure 10. Wear Coefficient Maps for R8T Wheel Material versus UIC60 900A Rail Steel

5. DISCUSSION

The aim of this work was to study wear regimes and transitions in wheel materials in order to provide a greater understanding of the wear mechanisms that could be used in improving wheel profile evolution modelling.

5.1 Wear Regimes and Mechanisms

In previous work an energy approach has been adopted in the analysis of the relationship between wear rate and contact conditions [13, 14, 15]. It was shown that wear rate ($\mu\text{g}/\text{m}$) is a linear function of wear index $T\gamma$ for the severe wear regime described earlier [15], where T is the tractive force and γ is the slip.

Wear data generated by Lewis & Dwyer-Joyce [18] has shown that at low $T\gamma$ conditions this relationship holds (see Figure 1). However, as shown in Figure 2, increasing the severity of the contact conditions causes the relationship to break down, as the transitions in wear rate occur.

Results of analysis of the wear transitions indicates that the relationship holds while partial slip conditions exist in the contact. When full slip conditions occur the wear rate levels off despite increasing slip values.

Further increases in the slip value then leads to temperatures in the contact that could cause a reduction in the wheel steel material properties, which could explain the subsequent increase in wear rate. This ties in with traditional theories of pure sliding wear that suggest that different wear mechanisms occur due to thermally induced changes in the properties of the surface layer material affected [25, 28]. It has been acknowledged that studies of wear types in rolling/sliding contacts have been carried far enough to draw such conclusions [29], so this work may act to fill this gap.

This improved understanding will help in progressing towards the aim of eventually attaining a wear modelling methodology reliant on material properties rather than wear constants derived from testing.

Data for a range of wheel/rail material combinations has been presented using two methods; wear rate versus $T\gamma$ plots and wear maps showing wear coefficients. The wear maps presented allow the contributions of sliding velocity and contact pressure to the wear rate to be isolated and give an understanding of where transitions occur between acceptable and more severe wear conditions. Relating expected pressure and slip in the wheel/rail contact is very important. It can help in determining:

- more efficient maintenance.
- where application of lubrication may be necessary to reduce wear problems.
- improving data input to simulation techniques used to predict wheel profile change.

5.2 Wear versus Wheel/Rail Contact Conditions

In previous work on wear of wheel steel no attempt has been made to correlate wear data to wheel/rail contact conditions. The wheel/rail contact conditions illustrated in Figure 11 resulted from a study using GENSYS train dynamic modelling software [30]. As can be seen a clear difference exists between the rail head/wheel tread and the rail gauge/wheel flange contacts.

To study how the wear regimes identified above fit in with the wheel/rail contact conditions, the wear map of R8T wheel steel versus UIC60 900A rail steel has been overlaid (from Figure 10). This indicates that the rail head/wheel tread contact will experience mild to severe wear and the rail gauge/wheel flange contact will experience severe to catastrophic wear. This backs up previous suppositions regarding the wear regimes that the rail head/wheel tread and rail gauge/wheel flange contacts fall into. Full-scale test results support this view [31]. The wheel flange wear was significantly higher compared with wheel tread wear. It could also be seen that the tread wear rate was higher for powered wheels than for trailing wheels.

Figure 12 shows the wear data points collected for the wheel materials in terms of the contact conditions. It can be seen that there is a large amount of wear test data for conditions typical of a rail head/wheel tread contact, but very little for the rail gauge/wheel flange contact. This clearly identifies an area that needs to be addressed in future research. Especially as axle loads are increasing and rolling stock is being used on track with low radius curves as well as the high radius curves on high speed lines, which means it is likely that the severity of the wheel/rail contact conditions will rise. Increasing the wear data available will also improve the accuracy and applicability of the wear maps.

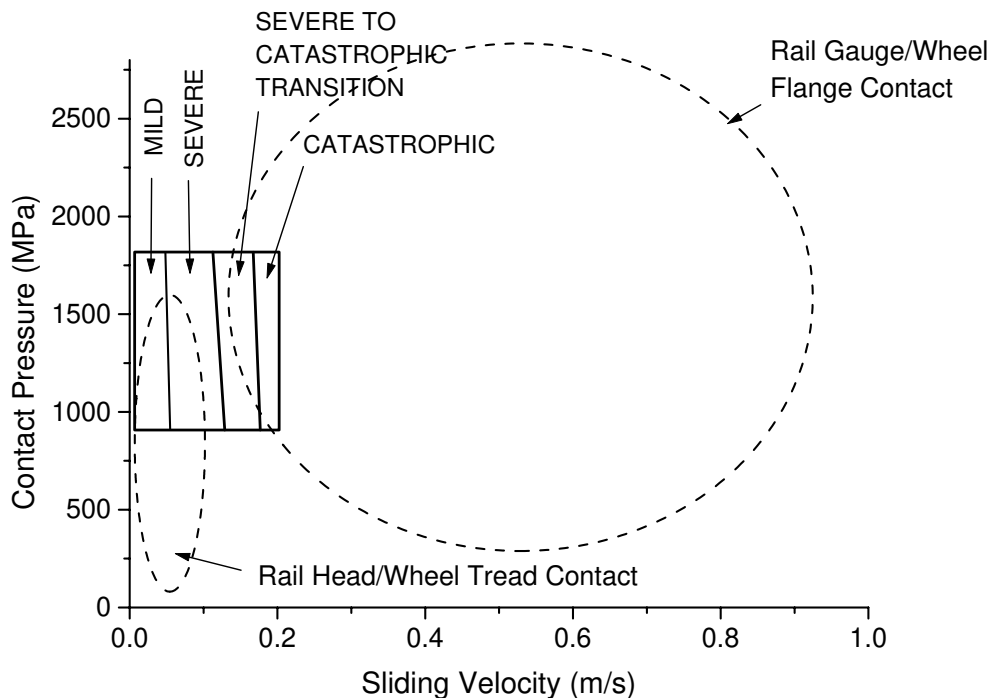


Figure 11. R8T Wheel Material Wear Map (from Figure 10) Plotted Over Wheel/Rail Contact Conditions Derived from GENSYS Simulations (Jendel, 2000b)

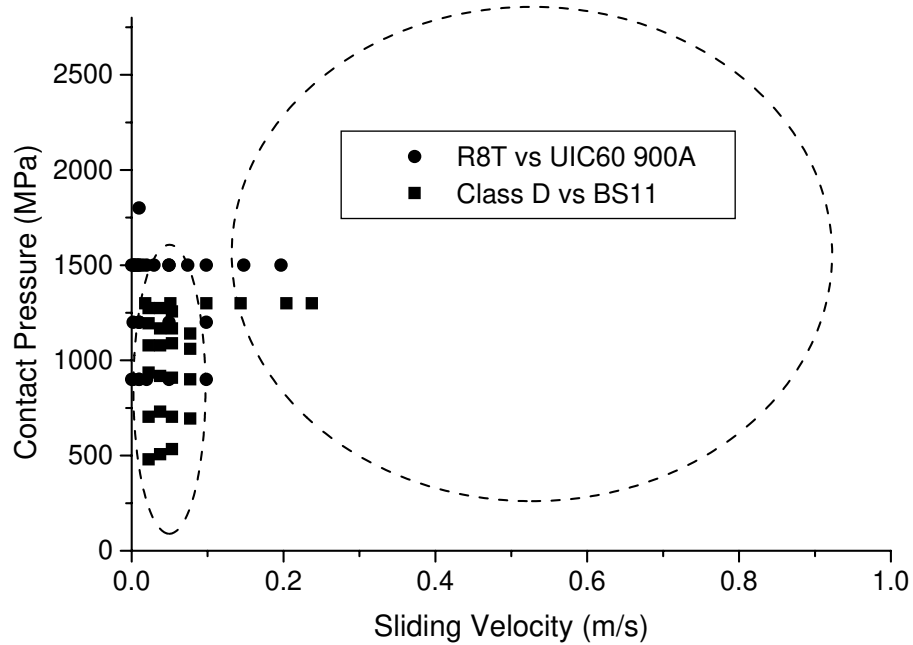


Figure 12. Available Wheel Material Wear Data Plotted Over Typical Wheel/Rail Contact Conditions

6. CONCLUSIONS

Three wear regimes have been identified for railway wheel materials; *mild*, *severe* and *catastrophic*. These were classified in terms of wear rate and features.

Mild wear is characterised by low wear rates and oxidative wear. Increasing the severity of the contact leads to cracking

Analysis of the contact conditions in terms of friction and slip indicated that the levelling off of the wear rate observed at the first wear transition was caused by the change from partial slip to full slip conditions at the disc interface.

Temperature calculations for the contact showed that the large increase in wear rates seen at the second wear transition may result from a thermally induced reduction in yield strength and other material properties.

Wear rates from twin disc testing have been related to actual wheel/rail contact conditions and show correlation with expected wear regimes in the tread and flange contact.

Gaps have been identified in current knowledge both in terms of wheel steel wear data and wear mechanisms that provide a focus for new research in this area.

7. REFERENCES

- [1] Stanca, M., Stefanini, A., Gallo, R., "Development of an Integrated Design Methodology for a New Generation of High Performance Rail Wheelsets", *Proceedings of the 16th European MDI User Conference*, Berchtesgaden, Germany, 14-15 November 2001.
- [2] Jendel, T., "Prediction of Wheel Profile Wear - Comparisons with Field Measurements", *Proceedings of the International Conference on Contact Mechanics and Wear of Rail/Wheel Systems*, Tokyo, Japan, 2000, pp117-124.
- [3] Fries, R.H., Dávila, C.G., "Wheel Wear Predictions for Tangent Track Running", *Transactions of the ASME, Journal of Dynamic Systems, Measurement, and Control*, Vol. 109, 1987, pp397-404.
- [4] Pearce T.G., Sherratt N.D., "Prediction of Wheel Profile Wear", *Wear*, Vol. 144, 1991, pp343-351.
- [5] Zobory, I. "Prediction of Wheel/Rail Profile Wear", *Vehicle System Dynamics*, Vol. 28, 1997, pp221-259.
- [6] Lewis, R., Dwyer-Joyce, R.S., Bruni, S., Ekberg, A., Cavalletti, M., Bel Knani, K., "A New CAE Procedure for Railway Wheel Tribological Design", accepted for presentation at the *14th International Wheelset Congress*, Florida, 17th-21st October 2004.
- [7] Telliskivi T., Olofsson U., "Contact mechanics analysis of measured wheel-rail profiles using the Finite Element Method", *Journal of Rail and Rapid Transit, Proceedings of the IMechE, Part F*, Vol. 215, 2001, pp65-72.
- [8] Telliskivi T., Olofsson U., "Wheel-Rail Wear Simulation", accepted for publication by *Wear*.
- [9] Dearden, J., "The Wear of Steel Rails and Tyres in Railway Service", *Wear*, Vol. 3, 1960, pp43-49.
- [10] Steele, R.K., "Observations of In-Service Wear of Railroad Wheels and Rails under conditions of widely varying Lubrication", *ASLE Transactions*, Vol. 25, No. 3, 1982, pp400-409.
- [11] McEwen, I.J., Harvey, R.F., "Full-scale Wheel-on-Rail Testing: Comparisons with Service Wear and a Developing Theoretical Predictive Model", *Lubrication Engineering*, Vol. 41, No. 2, 1985, pp80-88.

- [12] Kumar, S., Rao, D.L.P., "Wheel-Rail Contact Wear, Work, and Lateral Force for Zero Angle of Attack - A Laboratory Study", *Transactions of the ASME, Journal of Dynamic Systems, Measurement, and Control*, Vol. 106, 1984, pp319-326.
- [13] Beagley, T.M., "Severe Wear of Rolling/Sliding Contacts", *Wear*, Vol. 36, 1976, pp317-335.
- [14] Bolton, P.J., Clayton, P., McEwen, I.J., "Wear of Rail and Tyre Steels under Rolling/Sliding Conditions", *ASLE Transactions*, Vol. 25, No. 1, 1982, pp17-24.
- [15] Bolton, P.J., Clayton, P., "Rolling-Sliding Wear Damage in Rail and Tyre Steels", *Wear*, Vol. 93, 1984, pp145-165.
- [16] Krause, H., Poll, G., "Wear of Wheel-Rail Surfaces", *Wear*, Vol. 113, 1986, pp103-122.
- [17] Garnham, J.E., Beynon, J.H., "Dry Rolling-Sliding Wear of Bainitic and Pearlitic Steels", *Wear*, Vol. 57, 1992, pp81-109.
- [18] Lewis, R., Dwyer-Joyce, R.S., "Wear Mechanisms and Transitions in Railway Wheel Steels", submitted to *Journal of Engineering Tribology, Proceedings of the IMechE Part J*.
- [19] Broster, M., Pritchard, C., Smith, D.A., "Wheel-Rail Adhesion: It's Relation to Rail Contamination on British Railways", *Wear*, Vol. 29, 1974, pp309-321.
- [20] Carter, F.W., 1926, "On the Action of a Locomotive Driving Wheel", *Proceedings of the Royal Society*, Vol. A112, pp151-157.
- [21] Bower, A.F., Johnson, K.L., 1991, "Plastic Flow and Shakedown of the Rail Surface in Repeated Wheel-Rail Contact", *Wear*, Vol. 144, pp1-18.
- [22] Kapoor, A., "A Re-evaluation of the Life to Rupture of Ductile Metals by Cyclic Plastic Strain", *Fatigue and Fracture of Engineering Materials and Structures*, Vol. 17, 1994, pp201-219.
- [23] Blok, H., "The Flash Temperature Concept", *Wear*, Vol. 6, 1963, pp483-494.
- [24] British Steel Makers Creep Committee, *BSCC High Temperature Data*. The Iron and Steel Institute for the BSCC, London, 1973.
- [25] Lim, S.C., Ashby, M.F., "Wear Mechanism Maps", *Acta Metalllica*, Vol. 35, 1987, pp1-24.
- [26] Lewis, R., Olofsson, U., "Mapping Rail Wear Regimes and Transitions", accepted for publication by *Wear*.
- [27] Archard, J.F., "Contact and Rubbing of Flat Surfaces", *Journal of Applied Physics*, Vol. 24, 1953, pp981-988.
- [28] Rozeanu, L., "A Model for Seizure", *ASLE Transactions*, Vol. 16, 1973, pp115-120.
- [29] Markov, D., Kelly, D., "Mechanisms of Adhesion-initiated Catastrophic Wear: Pure Sliding", *Wear*, Vol. 239, 2000, pp189-210.
- [30] Jendel, T., "Prediction of Wheel Profile Wear – Methodology and Verification", Licentiate Thesis, TRITA-FKT 2000:9, Royal Institute of Technology, Stockholm, Sweden, 2000.
- [31] Nilsson R., "Wheel and Rail Wear – Measured Profiles and Hardness Changes during 2.5 years for Stockholm Commuter Traffic", *Proceedings of Railway Engineering – 2000*, London, England, 5-6 July, 2000.